

Supplementary information

High-energy O3-Na_{1-2x}Ca_x[Ni_{0.5}Mn_{0.5}]O₂ cathode for long-life sodium-ion batteries

Tae-Yeon Yu,^a Jongsoon Kim,^b Jang-Yeon Hwang,^c Hyungsub Kim,^d Geumjae Han,^a Hun-Gi Jung,^e and Yang-Kook Sun*^a

^aDepartment of Energy Engineering, Hanyang University, Seoul 04763, Republic of Korea

^bDepartment of Nanotechnology and Advanced Materials Engineering, Sejong University, Seoul 05006, Republic of Korea

^cDepartment of Materials Science and Engineering, Chonnam National University, Gwangju 61186, Republic of Korea

^dKorea Atomic Energy Research Institute, Daejeon 34507, Republic of Korea

^eCenter for Energy Storage Research, Green City Technology Institute, Korea Institute of Science and Technology, Seoul 02792, Republic of Korea

*Corresponding author: yksun@hanyang.ac.kr

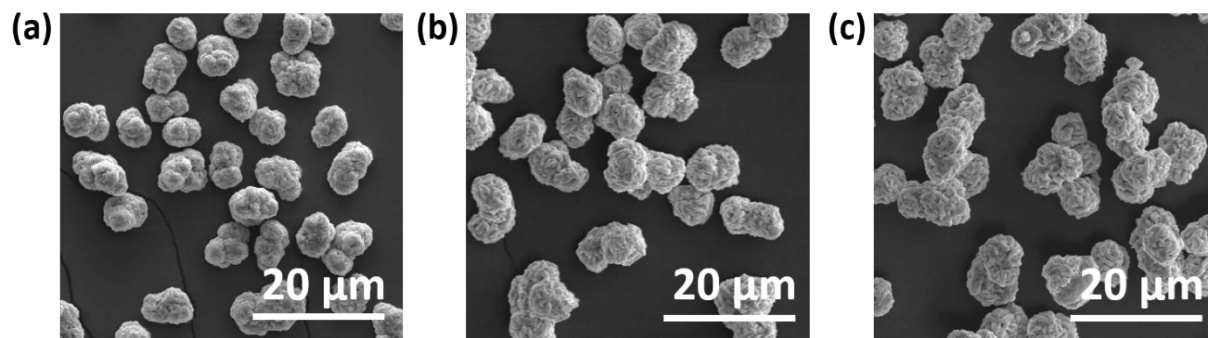


Fig. S1 SEM images of a) the $[\text{Ni}_{0.5}\text{Mn}_{0.5}](\text{OH})_2$ precursor, b) $\text{Na}[\text{Ni}_{0.5}\text{Mn}_{0.5}]\text{O}_2$, and c) Ca-substituted $\text{Na}_{0.98}\text{Ca}_{0.01}[\text{Ni}_{0.5}\text{Mn}_{0.5}]\text{O}_2$ cathodes at low magnification.

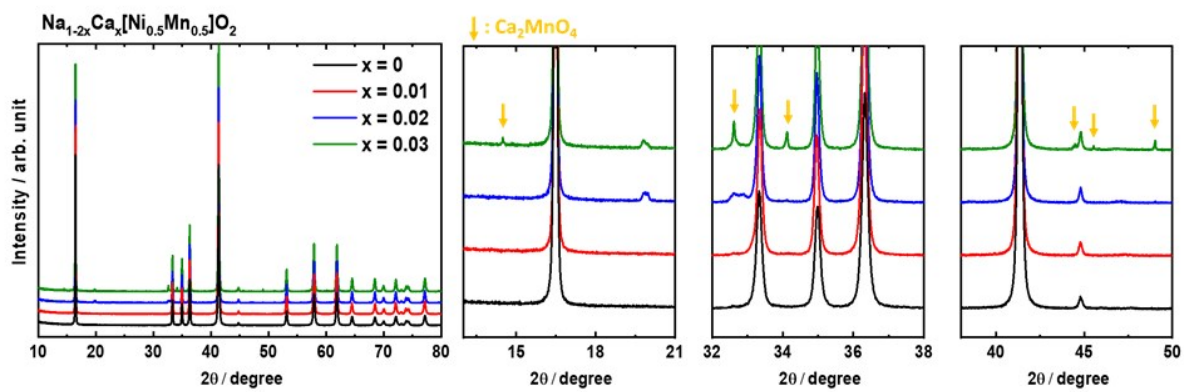


Fig. S2 Comparison of XRD patterns among various $\text{Na}_{1-2x}\text{Ca}_x[\text{Ni}_{0.5}\text{Mn}_{0.5}]\text{O}_2$ ($x = 0, 0.01, 0.02$ and 0.03) cathodes.

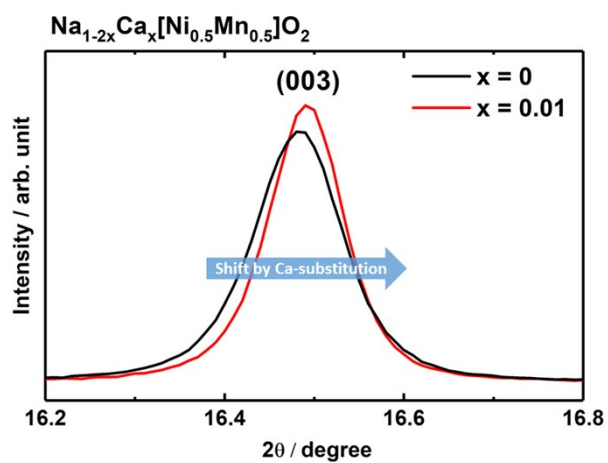


Fig. S3 Comparison of (003) XRD peak between pristine O3- $\text{Na}[\text{Ni}_{0.5}\text{Mn}_{0.5}]\text{O}_2$ and O3- $\text{Na}_{0.98}\text{Ca}_{0.01}[\text{Ni}_{0.5}\text{Mn}_{0.5}]\text{O}_2$ cathodes.

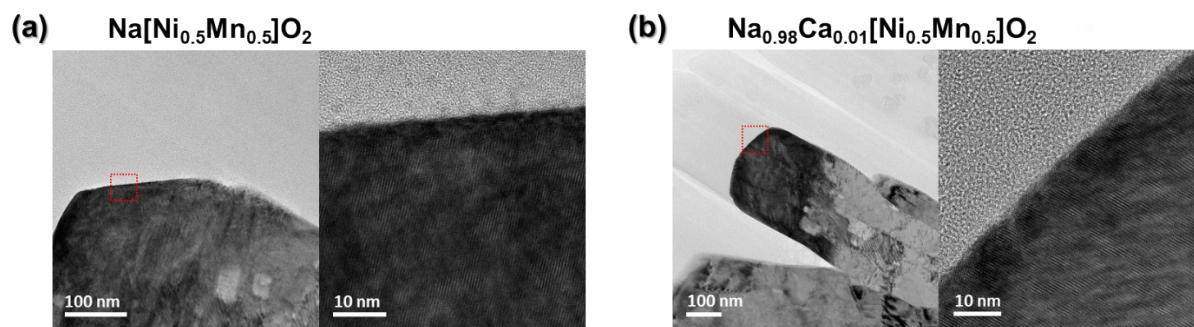


Fig. S4 Comparison of TEM images between pristine $\text{O3-Na}[\text{Ni}_{0.5}\text{Mn}_{0.5}]\text{O}_2$ and $\text{O3-Na}_{0.98}\text{Ca}_{0.01}[\text{Ni}_{0.5}\text{Mn}_{0.5}]\text{O}_2$ cathodes.

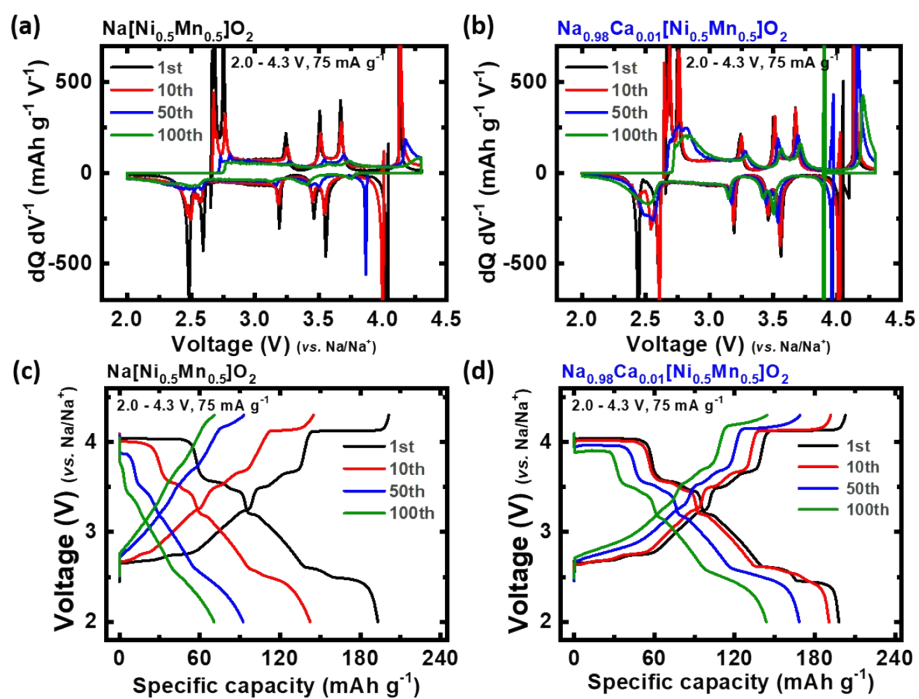


Fig. S5 dQ/dV versus V plots derived from consecutive cycling test at different cycle number for a) the $\text{Na}[\text{Ni}_{0.5}\text{Mn}_{0.5}]\text{O}_2$ and b) $\text{Na}_{0.98}\text{Ca}_{0.01}[\text{Ni}_{0.5}\text{Mn}_{0.5}]\text{O}_2$ cathodes. Corresponding charge-discharge voltage profiles for c) $\text{Na}[\text{Ni}_{0.5}\text{Mn}_{0.5}]\text{O}_2$ and d) $\text{Na}_{0.98}\text{Ca}_{0.01}[\text{Ni}_{0.5}\text{Mn}_{0.5}]\text{O}_2$ cathodes.

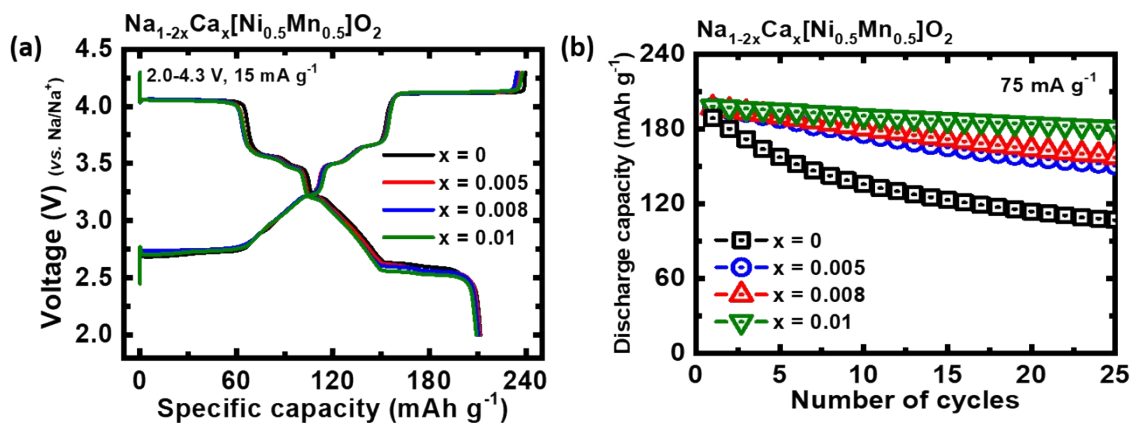


Fig. S6 Electrochemical performances of $\text{Na}_{1-2x}\text{Ca}_x[\text{Ni}_{0.5}\text{Mn}_{0.5}]\text{O}_2$ cathodes ($x = 0, 0.005, 0.008$ and 0.01) a) Charge-discharge profile at a current density of 15 mA g^{-1} . b) Cycling stability using 2032 coin-type cell at 75 mA g^{-1} , 30°C .

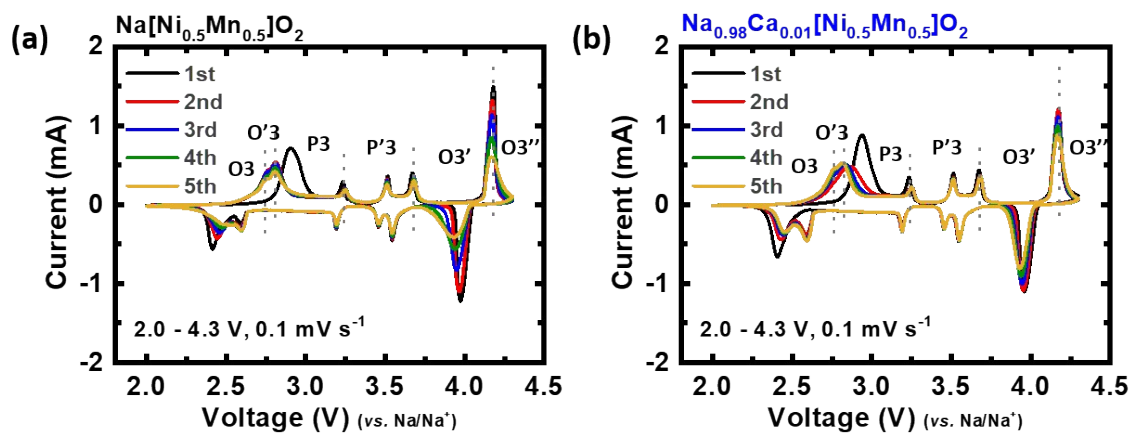


Fig. S7 CV plots at different cycle number for a) Na[Ni_{0.5}Mn_{0.5}]O₂ and b) Na_{0.98}Ca_{0.01}[Ni_{0.5}Mn_{0.5}]O₂ cathodes.

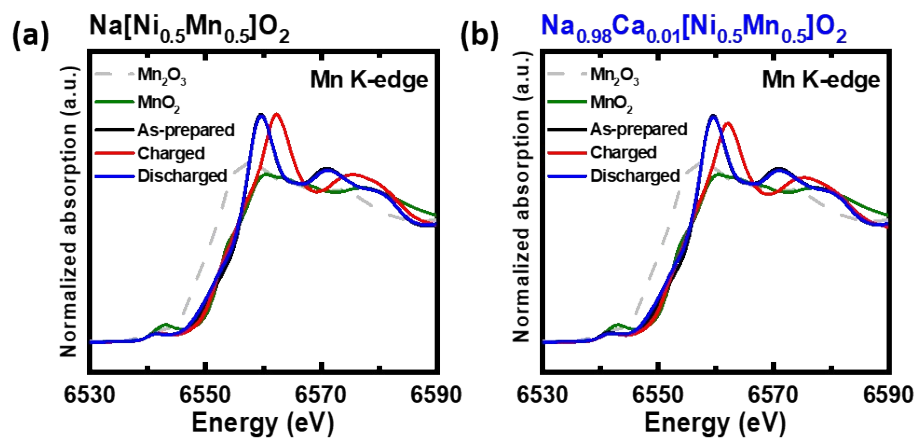


Fig. S8 *Ex-situ* XANES spectra at the Mn-K absorption edge of a) $\text{Na}[\text{Ni}_{0.5}\text{Mn}_{0.5}]\text{O}_2$ and b) $\text{Na}_{0.98}\text{Ca}_{0.01}[\text{Ni}_{0.5}\text{Mn}_{0.5}]\text{O}_2$ cathodes with Mn_2O_3 and MnO_2 spectra as the reference oxides.

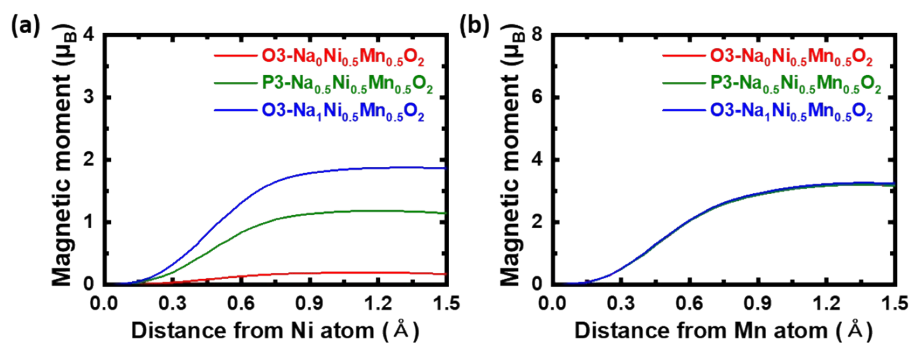


Fig. S9 The integrated spin moments of (a) Ni and (b) Mn ions among O3-Na₁[Ni_{0.5}Mn_{0.5}]O₂, P3-Na_{0.5}[Ni_{0.5}Mn_{0.5}]O₂ and O3-Na₀[Ni_{0.5}Mn_{0.5}]O₂.

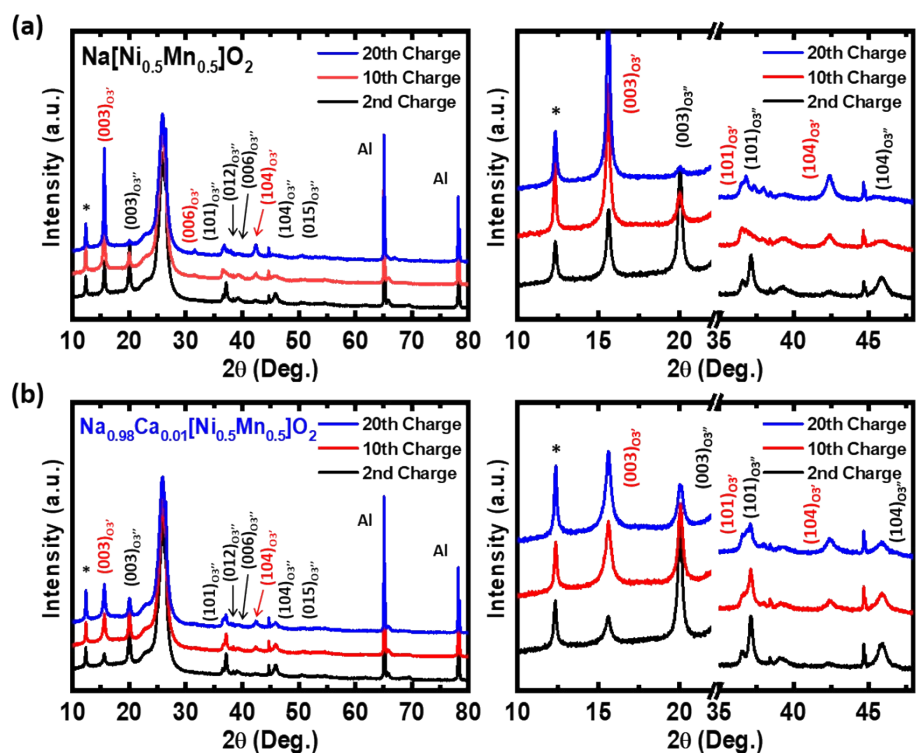


Fig. S10 Indexed *ex-situ* XRD patterns collected at several charge states of a) $\text{Na}[\text{Ni}_{0.5}\text{Mn}_{0.5}]\text{O}_2$ and b) $\text{Na}_{0.98}\text{Ca}_{0.01}[\text{Ni}_{0.5}\text{Mn}_{0.5}]\text{O}_2$ cathodes under a current density of 75 mA g^{-1} . The hydrated phase marked by *. The broad peak observed at $\sim 25^\circ$ is related to a Mylar film.

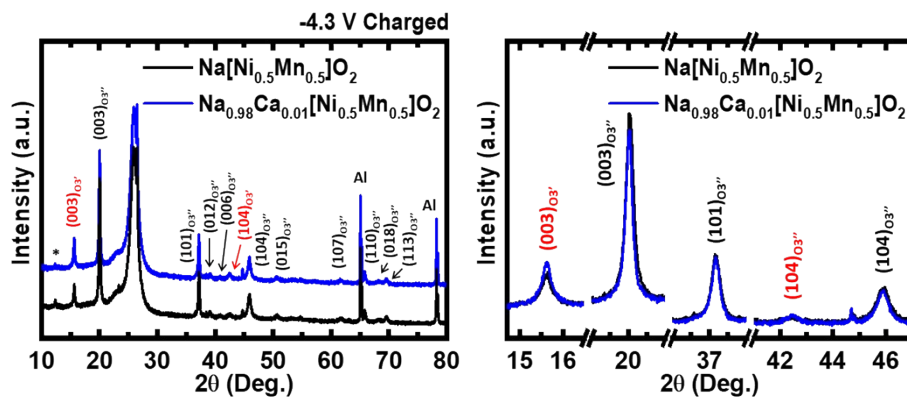


Fig. S11 Comparison of the indexed XRD patterns between $\text{Na}_x[\text{Ni}_{0.5}\text{Mn}_{0.5}]\text{O}_2$ and $\text{Na}_x\text{Ca}_{0.01}[\text{Ni}_{0.5}\text{Mn}_{0.5}]\text{O}_2$ (x is close to 0) electrodes charged to 4.3 V (vs. Na^+/Na). The hydrated phase marked by *. The broad peak observed at $\sim 25^\circ$ is related to a Mylar film.

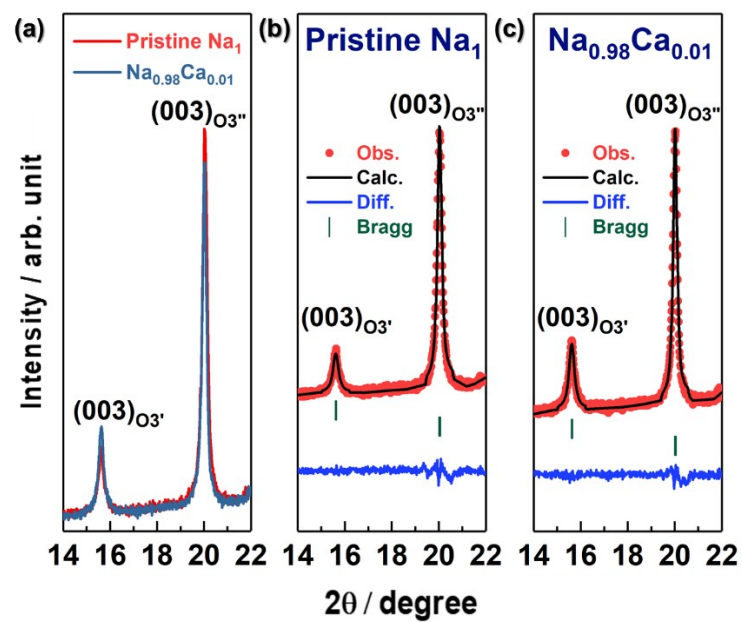


Fig. S12 (a) Comparison of the indexed XRD patterns between fully charged pristine $\text{Na}[\text{Ni}_{0.5}\text{Mn}_{0.5}]\text{O}_2$ and fully charged $\text{Na}_{0.98}\text{Ca}_{0.01}[\text{Ni}_{0.5}\text{Mn}_{0.5}]\text{O}_2$, and refined XRD patterns of (b) fully charged pristine $\text{Na}[\text{Ni}_{0.5}\text{Mn}_{0.5}]\text{O}_2$ and (c) fully charged $\text{Na}_{0.98}\text{Ca}_{0.01}[\text{Ni}_{0.5}\text{Mn}_{0.5}]\text{O}_2$.

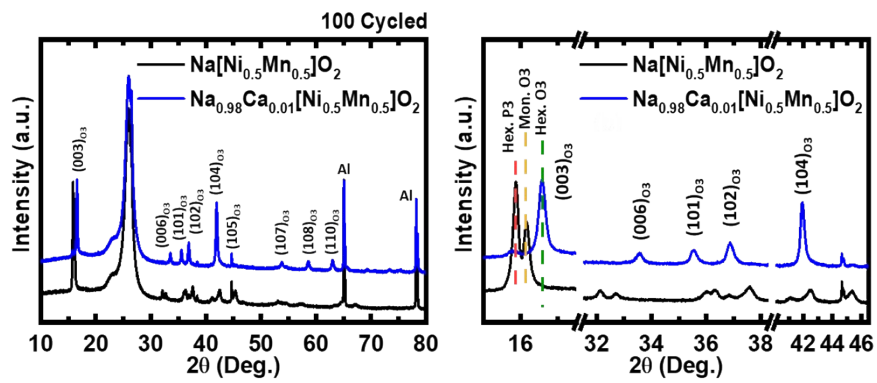


Fig. S13 Indexed *ex-situ* XRD patterns collected after 100 cycling of $\text{Na}[\text{Ni}_{0.5}\text{Mn}_{0.5}]\text{O}_2$ and $\text{Na}_{0.98}\text{Ca}_{0.01}[\text{Ni}_{0.5}\text{Mn}_{0.5}]\text{O}_2$ cathodes at 2.0-4.3V; Green line: Hex. O3 phase, Yellow line: Mon. O3 phase, Red line: Hex. P3 phase.

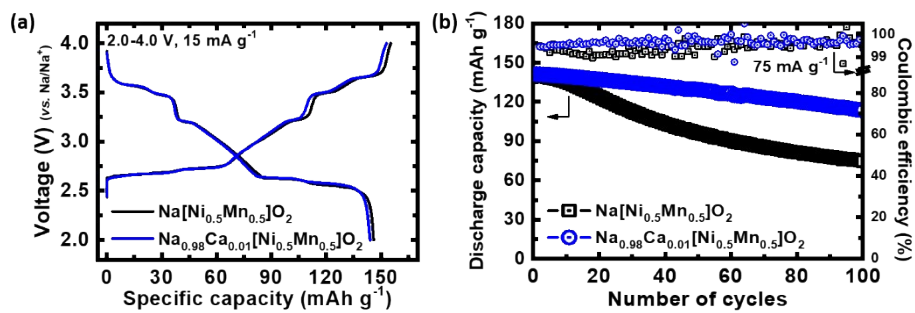


Fig. S14 Electrochemical performances of $\text{Na}[\text{Ni}_{0.5}\text{Mn}_{0.5}]\text{O}_2$ and $\text{Na}_{0.98}\text{Ca}_{0.01}[\text{Ni}_{0.5}\text{Mn}_{0.5}]\text{O}_2$ cathodes in the voltage range of 2.0-4.0 V. a) Charge-discharge profile at a current density of 15 mA g^{-1} . b) Cycling stability at 75 mA g^{-1} , 30°C .

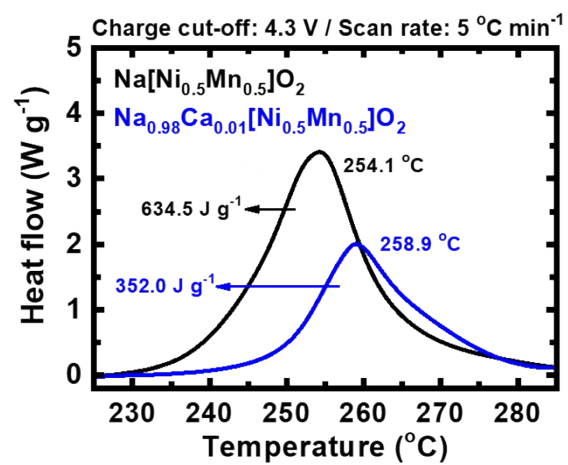


Fig. S15 Differential scanning calorimetry (DSC) data for de-sodiated Na_x[Ni_{0.5}Mn_{0.5}]O₂ and Na_xCa_{0.01}[Ni_{0.5}Mn_{0.5}]O₂ (x is close to 0) cathodes.

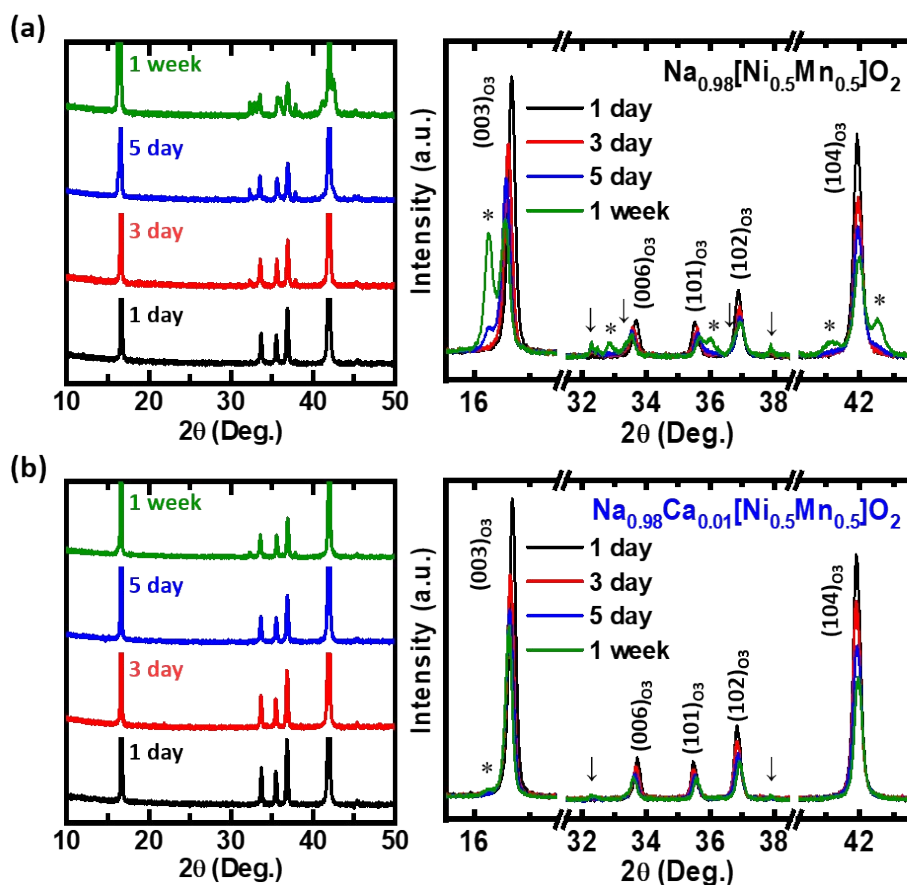


Fig. S16 Evolution of XRD patterns of a) $\text{Na}[\text{Ni}_{0.5}\text{Mn}_{0.5}]\text{O}_2$ and b) $\text{Na}_{0.98}\text{Ca}_{0.01}[\text{Ni}_{0.5}\text{Mn}_{0.5}]\text{O}_2$ cathodes within 1 week storage in relative humidity $\approx 55\%$ environment. $\text{Na}_2\text{CO}_3 \cdot n\text{H}_2\text{O}$ was indexed by \downarrow in XRD patterns, which was probably formed by the reaction of Na^+ ion diffused out of the structure with humid air. The transformed monoclinic phase marked by *.

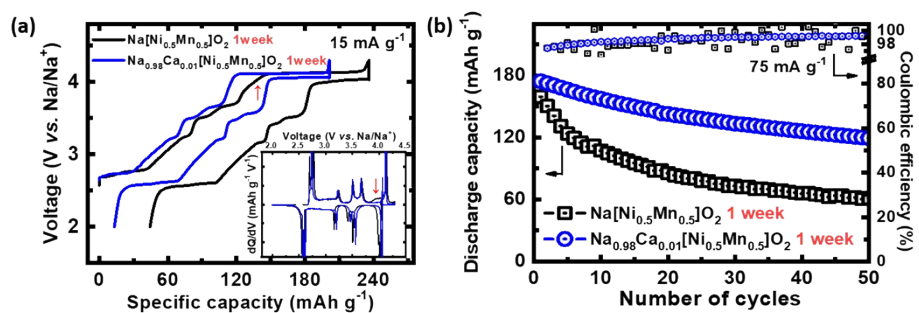


Fig. S17 Electrochemical performances of $\text{Na}[\text{Ni}_{0.5}\text{Mn}_{0.5}]\text{O}_2$ and $\text{Na}_{0.98}\text{Ca}_{0.01}[\text{Ni}_{0.5}\text{Mn}_{0.5}]\text{O}_2$ cathodes after 1 week of exposure to air with Relative Humidity $\approx 55\%$. a) Charge-discharge profile at a current density of 15 mA g^{-1} and $dQ dV^{-1}$ versus V plots (inset figure). For the exposure $\text{Na}[\text{Ni}_{0.5}\text{Mn}_{0.5}]\text{O}_2$, there is a new reaction marked by \downarrow due to the decomposition of Na_2CO_3 . b) Cycling test at 75 mA g^{-1} , 30°C .

Table S1. ICP-OES results of $\text{Na}_{1-2x}\text{Ca}_x[\text{Ni}_{0.5}\text{Mn}_{0.5}]\text{O}_2$ ($x = 0 - 0.03$) series.

Metal stoichiometry determined by ICP-OES				
Sample	Na	Ca	Ni	Mn
$\text{Na}[\text{Ni}_{0.5}\text{Mn}_{0.5}]\text{O}_2$	0.9975	0.0000	0.4943	0.5057
$\text{Na}_{0.98}\text{Ca}_{0.01}[\text{Ni}_{0.5}\text{Mn}_{0.5}]\text{O}_2$	0.9803	0.0099	0.4989	0.5011
$\text{Na}_{0.96}\text{Ca}_{0.02}[\text{Ni}_{0.5}\text{Mn}_{0.5}]\text{O}_2$	0.9512	0.0194	0.4936	0.4964
$\text{Na}_{0.94}\text{Ca}_{0.03}[\text{Ni}_{0.5}\text{Mn}_{0.5}]\text{O}_2$	0.9295	0.0278	0.4975	0.4927

Table S2. Lattice parameters deduced from the XRD Rietveld refinement within the $R\bar{3}m$ space group for $\text{Na}[\text{Ni}_{0.5}\text{Mn}_{0.5}]\text{O}_2$.



Lattice parameters			a (Å) = 2.96123 (3), c (Å) = 15.9244 (2)			
$R_p = 6.85 \%$		$R_{wp} = 8.79 \%$	$R_I = 3.55 \%$		$R_F = 2.11 \%$	
Site	x	y	z	B_{iso}	Occ	
Na1	0	0	0	1.52 (2)	1	
Ni1	0	0	0.5	0.58 (1)	0.5	
Mn1	0	0	0.5	0.58 (1)	0.5	
O1	0	0	0.23177 (5)	0.71 (2)	1	

Table S3. Lattice parameters deduced from the XRD Rietveld refinement within the $R\bar{3}m$ space group for $\text{Na}_{0.98}\text{Ca}_{0.01}[\text{Ni}_{0.5}\text{Mn}_{0.5}]\text{O}_2$.



Lattice parameters			a (Å) = 2.96282 (2), c (Å) = 15.9152 (2)			
$R_p = 6.58 \%$	$R_{wp} = 8.82 \%$		$R_l = 2.98 \%$	$R_F = 1.85 \%$		
Site	x	y	z	B_{iso}	Occ	
Na1	0	0	0	1.11 (2)	0.98	
Ca1	0	0	0	1.11 (2)	0.01	
Ni1	0	0	0.5	0.34 (1)	0.5	
Mn1	0	0	0.5	0.34 (1)	0.5	
O1	0	0	0.23226 (4)	0.59 (2)	1	

Table S4. Rietveld refinement Results on the XRD patterns of fully charged pristine $\text{Na}[\text{Ni}_{0.5}\text{Mn}_{0.5}]\text{O}_2$ and fully charged $\text{Na}_{0.98}\text{Ca}_{0.01}[\text{Ni}_{0.5}\text{Mn}_{0.5}]\text{O}_2$.

	$\text{Na}[\text{Ni}_{0.5}\text{Mn}_{0.5}]\text{O}_2$		$\text{Na}_{0.98}\text{Ca}_{0.01}[\text{Ni}_{0.5}\text{Mn}_{0.5}]\text{O}_2$	
	O3'	O3''	O3'	O3''
c-lattice parameter (Å)	17.020 (3)	13.2919 (4)	17.018 (2)	13.2982 (3)
Phase-proportion (%)	12.24 (5)	87.76 (13)	19.48 (6)	80.52 (11)